Chapter

Vacuum-Free Fabrication of Transparent Electrodes for Soft Electronics

Arshad Khan, Shawkat Ali, Saleem Khan, Moaaz Ahmed, Bo Wang and Amine Bermak

Abstract

Optoelectronic devices are advancing from existing rigid configurations to deformable configurations. These developing devices need transparent electrodes (TEs) having high mechanical deformability while preserving the high electrical conductivity and optical transparency. In agreement with these requirements, vacuum-fabricated conventional TEs based on transparent conducting oxides (TCOs) are receiving difficulties due to its low abundance, film brittleness, and low optical transmittance. Novel solution-processed TE materials including regular metal meshes, metal nanowire (NW) grids, carbon materials, and conducting polymers have been studied and confirmed their capabilities to address the limitations of the TCO-based TEs. This chapter presents a comprehensive review of the latest advances of these vacuum-free TEs, comprising the electrode material classes, the optical, electrical, mechanical and surface feature properties of the soft TEs, and the vacuum-free practices for their fabrication.

Keywords: fabrication, transparent electrodes, solution processed, soft electronics, stretchable electronics

1. Introduction

Nanofabrication means the manufacturing techniques of material or structures with critical dimensions in range of one to few hundreds of nanometers. These techniques realizes exceptionally small, features, structures, devices and systems those have applications in numerous fields of basic and applied sciences. It is comparatively a new class of manufacturing that signifies recent areas of sciences as well as creates new markets. Unlike conventional fabrication approaches, research in nanofabrication is multidisciplinary and needs combined work crosswise conventional fields. In nanofabrication, the final product is based on nanoscale materials, such as powders or fluids, and the components are realized either in "bottom up" or "top down" fashion, using various nanotechnologies. Similar to other fields, the applications of nanofabrication approaches are enormous in optoelectronic devices, [1] for instance, solar cells, [2] smart windows, [3] light-emitting diodes, [4] displays, [5] transparent sensors, [6] and touchscreens. [7] Transparent electrodes (TEs) are the key components in such optoelectronic devices. In addition to high optical transmittance and low sheet resistance [8] required for traditional TEs, next-generation soft optoelectronic devices also need decent mechanical deformability [1, 9] in TEs. Currently, the most utilized TEs are based on vacuum-processed TCOs, comprising fluorine-doped tin oxide and indium tin oxide (ITO). [10, 11] Although TCOs based TEs have demonstrated the required optoelectronic performance, several limitations, such as low abundance, [12] film brittleness, [13] low infrared transparency, [14] and failure during high temperature sintering, undermine their appropriateness for utilization in the future soft optoelectronic systems. Thus, researchers have developed novel TE materials and vacuum-free approaches for its fabrication to substitute the TCOs. [15, 16]

Novel intrinsically transparent materials including graphene, [17] carbon nanotubes (CNTs), [18] and conducting polymers [19, 20] have been explored to replace the TCOs. Besides, other promising class of soft TEs designed from metals are widely employed due to their excellent electrical, optical, and mechanical performance. This typically include metal NWs networks [21, 22] and systematic metal meshes, [23–28] and ultra-thin metal films. [29–31] In addition to the advancement of new materials for soft TEs, plenty of research is performed on the development of vacuum-free technologies for the low-cost fabrication of soft TEs. The list of these techniques is mainly consists of spin coating, [32] spray deposition, [33] inkjet printing, [34] screen printing, [35] transfer printing, [36] and slot-die coating. [37]

There have been several reviews published over the years, aiming at soft TEs from applications perspective. [1, 11, 38] However, few of them focuses on the soft TEs from the fabrication perspective. In this chapter, latest review of the vacuum-free fabricated TEs for emerging soft electronic devices is presented. The chapter begins with the discussion of key properties of TEs for soft electronics (sections 2). We then introduce the TE materials including metals, carbon materials, and transparent conducting polymers (section 3,4). Finally in section 5, the recent progress on vacuum-free methods that are typically employed for the realization of TEs, discussing their merits and demerits. We hope this chapter will enlighten the readers about the emergent soft TEs to better design and fabricate low-cost soft electronics devices.

2. Important properties of the soft transparent electrodes

2.1 Optical transmittance and electrical conductivity

Preferably, TEs must exhibit both high optical transmittance and high electrical conductance, and these are rather contrary from the physics perspective. It is due to an essential requirement for the electrical conductance of a material is the high charge density, that is restricted via the optical absorption of the free charges. [9] Figure of merit (FoM) is commonly used for evaluation of the overall performance of the transparent electrodes. FoM, which is the proportion of electrical conductivity to optical conductivity (σ_{dc}/σ_{opt}), and is measured by means of the commonly used expression, as given below: [20, 22, 25, 26].

$$\mathrm{FoM} = \frac{\sigma_{dc}}{\sigma_{opt}} = \frac{188.5}{R_s\left(\frac{1}{\sqrt{T}} - 1\right)} \tag{1}$$

Where, T represents the optical transparency value at a wavelength of 550 nm (as it is close to most sensitive wavelength of the human eyes, [39]) and R_s represents the sheet resistance. A larger FOM value discloses a smaller sheet resistance value at a particular optical transmittance value, and vice versa. **Figure 1** presents a comparison of FoMs for metallic soft TEs reported in recent studies. Among

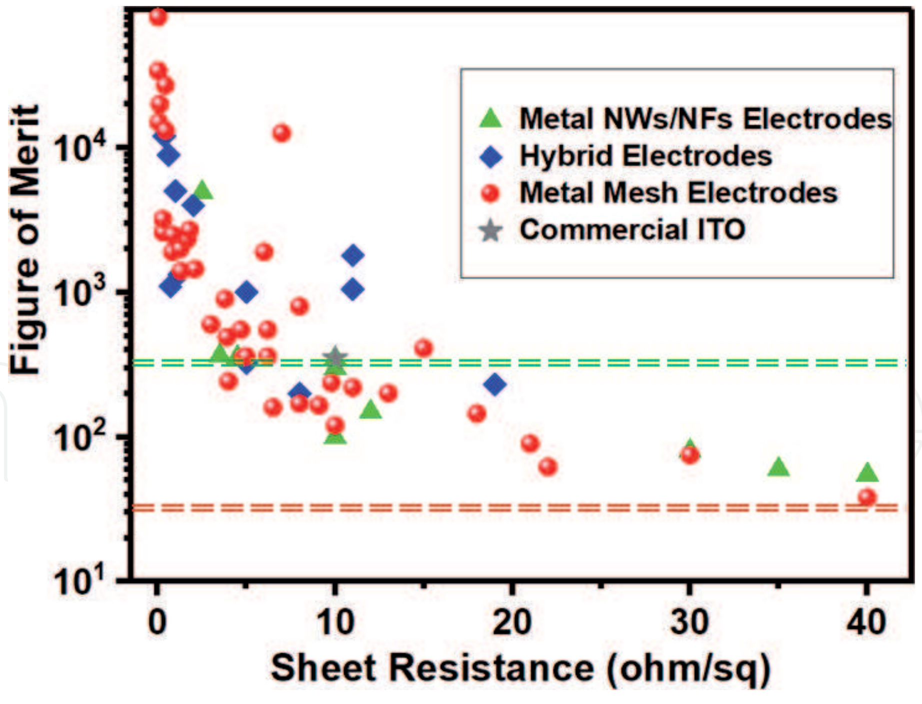

Figure 1.
Comparison of the FoMs of soft TEs (metal NW, metal mesh, and hybrid) and industrial standards. The data was acquired from the literature. [15] The dashed lines represent typical industrial standard (green line) and minimum industrial standard (red line). [40].

these classes, metal-mesh based TEs has higher FoM values, both alone and as part of the hybrid TEs. The detailed FoM values of metal based TEs are presented in **Tables 1–3**.

2.2 Mechanical stability

Mechanically resilient TEs remarkable optoelectronic properties are vital for the development of soft optoelectronic devices as without this, these systems will

R_{sh} (Ω-□$^{-1}$)	T (%)	FoM	Applications	Reference
40	85	55	Low-cost TEs	[41]
35	84	60	Low-cost TEs	[42]
6.2	85	360	Low-cost TEs	[43]
10	70	100	GaN-based LEDs	[44]
12	82	150	OLEDs	[45]
4.5	80	357	Photodetectors	[46]
10	89	300	Touch-screens	[47]
92	92	40	Touch-screens	[48]
3.5	76	366	Low-cost TEs	[49]
10	90	350	Large-area TEs	[50]
2.5	97.3	4920	High-performance TEs	[51]
130.5	92	35	Touch-screens	[52]
30	85	80	OSCs	[53]

Table 1.
Optical and electrical performance, and applications of metal NWs based soft TEs published in recent literature.

R_{sh} (Ω-□$^{-1}$)	T (%)	FoM	Applications	Reference
0.036	75	34000	DSSCs/Heaters	[15]
4	70	242	OLEDs	[54]
15	96	410	Touch-screens	[24]
21	85	90	Stretchable TEs	[55]
40	80	38	OFETs/ OLEDs/OSCs	[56]
22	78	62	OSCs	[57]
30	85	75	Touch-screens	[23]
3	82	600	Transparent Heaters	[58]
8	77	170	OSCs	[59]
0.3	70	3200	Large-area TEs	[27]
1.7	82	2700	EL displays	[60]
0.03	86	80,000	Transparent Heaters	[61]
4.8	81	355	Printed TEs	[62]
18	76	145	High-durable TEs	[26]
5	82	360	Touch-screens	[25]
9.8	85.2	237	Touch-screens	[63]
6	97	1900	Transparent Heaters	[64]
8	94	800	Printed TEs	[65]
7	96	12600	Nanofiber based TEs	[66]
0.43	97	27000	Wearable TEs	[67]
0.07	72	15000	Transparent Heaters	[16]
0.13	86	20000	Transparent Heaters	[68]
1.32	82	1400	DSSCs	[69]
0.84	84	2500	EL displays	[70]
3.8	90	900	Wearable Heaters	[71]
2.1	88.6	1450	QLEDs	[72]
13	87	200	Touch-screens	[73]
10	75	120	Solar Cells	[74]
11	86	220	Transparent Heaters	[75]
4.7	87	550	OLEDs	[76]
6.2	90	550	Transparent Heaters	[77]
3.9	84	490	Highly Bendable TEs	[78]

Table 2.
Optical and electrical performance, and applications of regular metal mesh based soft TEs published in recent literature.

not be not able to preserve electrical conductivity under significant mechanical deformation. [69] Various approaches are developed to enhance the mechanical stability of the soft TEs. For example, metal meshes are embedded and mechanically anchored into the soft polymer substrates, which significantly enhanced its adhesion with the substrate and as a result improves its mechanical stability under deformation. [15, 16, 86] In addition to the mechanical stability of the TEs, the

R_{sh} (Ω-□$^{-1}$)	T (%)	FoM	Applications	Reference
1	92	5000	High-performance TEs	[40]
2	95	4000	High-performance TEs	[40]
1.2	80	1330	OSCs	[79]
19	92	232	Perovskite Solar Cells	[80]
9.1	79	165	OSCs	[81]
5	80	325	Long-term Stable TEs	[82]
0.6	93	8900	High-performance TEs	[40]
0.36	92	12000	E-chromic Devices	[83]
0.7	65	1100	Stretchable TEs	[55]
11	98	1800	High-performance TEs	[84]
3	92	1400	High-performance TEs	[84]
60	90	60	PLEDs	[85]
11	88	1050	Stretchable TEs	[55]

Table 3.
Optical and electrical performance, and applications of hybrid soft TEs published in recent literature.

intrinsic mechanical stability of the other functional materials are equally important concerning the successful operations of the soft electronic devices.

2.3 Other surface properties

TEs Surface roughness is significant as this considerably influences the morphology and uniformity of the subsequent printed/coated layers. Though, it's hard to define a strict extreme roughness value vital for the effective production of soft electronic devices. Yet, bottom TEs with lower surface roughness value are preferred to minimize the possibility of electrical short circuiting. For instance, the roughness (root-mean-square) of a coated/printed continuous PEDOT:PSS film is normally <10 nm, which is adequately flat for most of the functional thin-films involved in fabrication of electronic devices. But, the surface roughness of metal TEs is much higher (hundreds of nm to few μm). For example, screen printed silver mesh is >2 μm thick, making the subsequent functional layer uniform deposition impossible. [87] To address this, researchers have has embedded the metal-mesh into the polymer substrates to flat the TEs top surface. [16, 69] Similarly, metal NW networks also demonstrate decent FoM as stated above, however, its high roughness resulted in poor device performance. [88] Therefore, multiple approaches have been established to flatten the metal NWs TEs by compacting the unattached networks to a dense structure or filling the openings with supplementary TE materials. [89, 90]

Chemical compatibility of the TEs/functional materials interface is another important concern for TEs. An unsteady interface can cause substandard performance and also fast deprivation of the TEs. For instance, the acidic behavior of PEDOT:PSS TEs can corrode the base ITO layer, causing the diffusion of indium at the TE/active layer boundary. Such erosion might result in critical gap conditions which further caused the degradation of device. [91] To minimize the risk of chemical/electrochemical decay of the sensitive metallic TEs, a traditional method is covering the sensitive metallic materials with a thin-film. [92] This thin-film can be either from another class of conductor, for example, graphene, [93] and less-sensitive metals, [94] or an insulating material, for instance, poly(methyl methacrylate) (PMMA) and alumina, [95] The insulating film must be ultra-thin (< few nanometers) for proficient charge transport. [96] In addition to roughness and chemical compatibility, surface energy of TEs is also an essential factor to be considered for the efficient performance of the active materials in soft electronic devices. [97]

3. Metal based soft TEs

Due to the high density of free electrons, metals demonstrate the uppermost electrical conductance among all the conductive materials. Yet, metallic materials in bulk are unable to work as TEs directly as it has high light reflection at visible wavelength. [11] Thus, shape structuring is essential for metallic materials to attain the required optoelectronic characteristics. Following are the classes of metal-based TEs frequently reported in recent years. These typically include metal nanoparticle/nanowire/nanofiber networks, regular metal meshes, and ultra-thin metal films.

3.1 Metal nanoparticle/nanowire/nanofiber networks

One of the major classes of soft TEs is prepared from the metal NPs/NWs networks [21, 22], that have exhibited enormous performance in optical transparency, electrical conductivity, and mechanical deformation. The metal NPs or NWs must be gathered to form transparent metal meshes using several vacuum-free fabrication methods to realize soft TEs. In reality, the porous arrangement of these class of TEs permit the light to go across the free spaces in the grids. Therefore, the electrical and optical conductivity of these electrodes are greatly reliant on the grid arrangement. Simply, the electrical conductance depends on the density of metallic materials, while the optical transmittance is determined by the area fraction of metal coverage. Among these, TEs prepared from the metal NWs got much attention because of their shape and that they can easily be dispersed in various solvents. Therefore, these can be processed by multiple vacuum-free techniques to create TEs having decent optoelectronic performance for soft electronic applications. **Table 1** reviews the electrical and optical performance, and applications of metal NWs based soft TEs published in recent literature. Similar to other classes, metal NWs soft TEs also suffer from quite a few difficulties such as problem in achieving smooth NWs distribution across the large-area substrates, and the NWs delamination from the substrate during deformation. [9] In addition, the dispersed NWs network cannot be employed directly as further processing steps are normally required to eliminate the polymer capping around the NWs to decrease the junction resistance. This is achieved either using selective welding, bulk heating, or chemical processes. In addition to metal NWs, nanofiber based TEs have also got great interest due to their wide range of unique capabilities. Nanofibers are fabricated by employing various approaches, however, electrospinning technique is considered to be facile and low-cost to realize nanofibers with decent reproducibility, well-controlled shape, high aspect ratio, and saleable size. Moreover, the production of nanofibers can be enhanced by means of electrospinning system with multi-nozzles. [98] Despite this potential, TEs based on nanofibers [24, 67, 84, 99] have the randomly distributed patterns and because of this, the reproducibility of placing the nanofibers in precise locations and alignments remains a foremost challenge in these TEs. [15, 100]

3.2 Regular metal meshes

Compared with metal NPs/NWs, metal-mesh based soft TEs look extra proficient as their electrical and optical conductivity can easily be adjusted in a broad assortment via changing the line width, mesh opening, and thickness. [26] Besides, numerous metals can be employed as metal-mesh based TEs to attain the desired chemical characteristics and work functions for the targeted soft electronic applications. [24] **Table 2** summarizes the electrical and optical performance, and applications of metal mesh based soft TEs published in recent literature. The presented data shows that the FoM values of metal-mesh based TEs are comparatively higher than that of metal NPs/NWs based TEs. This is mainly due to the low junction resistances, offered by the regular metal meshes. Regardless of the superior performances, rough surface topography and poor adhesion between the meshes and substrates constrained the extensive use of metal-mesh based TEs in soft electronic industry.

3.3 Transparent thin metal films

Mostly, bulk metallic films having tens to hundreds of nanometers thicknesses are utilized as back-electrodes (opaque-cathodes). But, ultra-thin metal films with only few nanometers thicknesses can also be utilized as front-electrodes (transparent-anodes). Since, these metal layers are thinner in comparison with the light visible wavelength, and thus are optically transparent to human-eye. The thickness and uniformity of the metal films determine the optoelectronic performance of these TEs for the desired soft electronic applications. Several metals having different work-functions, including silver, nickel, gold, and platinum are effectively employed as transparent electrodes in soft electronic devices. [100] However, the vacuum-free fabrication of these ultra-thin transparent metallic films over large area is difficult, and thus substantial advancements in the fabrication methods are required to efficiently mass-produce these thin metal films.

4. Other soft TEs

4.1 Carbon materials

Graphene: Graphene efficiently conducts electricity and heat, is stronger than steel (~200 times), and is nearly transparent. [101] Due to these unique characteristics, it has been suggested as a substitute soft TE material. Over the years, various vacuum-free approaches are established to produce thin films of graphene on soft substrate materials. [102–104] Recently, significant advancement has been made to enhance the optoelectronic properties of the graphene based TEs. Large-area graphene film was made-up on copper catalyst (~30 inches diagonal size), which was then accurately transferred to the target soft substrate using transfer printing technique. [105] In an ideal world, graphene has massive capability and is currently offering the assurance of being the vital transparent material for soft TEs. However as a matter of fact, uniform ultra-thin films of graphene are exceedingly challenging and are costly to produce. In addition, optoelectronic performances of graphene based TEs reduce quickly, due to the wrinkles/folds and crystallographic defects formed in these ultra-thin films during mechanical deformation. [105, 106]

Carbon Nanotubes: Similar to graphene, CNT is one of the hardest materials recognized. Due to its decent electronic and mechanical characteristics, CNTs are productively employed as TE material in soft electronic devices. [107–110]

Numerous vacuum-free approaches, for example, spin coating [111] and transfer printing, [112] are developed to produce CNTs based soft TEs. While, CNTs based TEs have attractive characteristics, such as higher optical transmittance and superior mechanical deformation capability, these have typically poor electrical conductivity. This limitation makes CNTs less suitable for large-area commercial soft electronics.

4.2 Transparent conducting polymers

PEDOT:PSS: Few transparent polymers, having intrinsically poor electrical conductivity, are transformed into conducting polymers via addition of conductive dopants into their iterating chains. Poly (3,4-ethylenedioxythiophene) polystyrene sulfonate (PEDOT:PSS) is one of the classic model of such conducting polymers. In PEDOT: PSS unit chain, PEDOT acts as the conducting polymer, while the PSS plays the role of a dopant, enhancing its electrical conductance via significantly increasing the charge carriers. Since, PEDOT:PSS has no visible absorptive resonances, therefore it is routinely used as TEs in small scale soft electronic devices. Yet, a number of concerns, for example, instable molecular structure and high water solubility have limited the use of PEDOT:PSS in large-scale soft electronics. [113, 114]

Other Conducting Polymers: Besides PEDOT:PSS, other conducting polymers comprising poly(p-phenylene-vinylene) (PPV), polyaniline (PANI), polyfuran (PF), polypyrrole (PPy), are utilized as TE materials for several soft electronic devices, due to their decent electrical and optical conductivity. [115, 116]

As discussed above, each class of soft TEs offers unique set of favorable properties, and also has some disadvantages. Researchers have combined different classes of TEs into a single electrode structure to fabricate hybrid soft TEs. The objectives of developing this new class TEs are: (1) take advantage of the benefits offered by individual electrode. (2) overcome those challenges associated with the electrode once employed individually. **Table 3** summarizes, the optical and electrical performance, and applications of hybrid soft TEs published in recent literature.

5. Vacuum-free fabrication approaches for soft TEs

Vacuum-free thin film fabrication techniques are favored by soft electronic industry because of low cost, low material waste and high output as compared with conventional vacuum fabrication processes. Yet, accomplishing equivalent quality solution-processed TEs is a challenging job due to several reasons, including the substrate/TE adhesion, the solvent volatility, surface wettability, and solution rheology need to be accustomed. Following are the most commonly reported vacuum-free printing and coating approaches for the fabrication of soft TEs.

5.1 Spin coating

It is a simple technique used to coat continuous thin films onto rigid flat surfaces. Typically a small amount of coating material is put on the substrate's center, that is ideally spinning at low speed. The substrate is then rotated at high speed (max ~10 k rpm) to uniformly spread the coat-material utilizing the centrifugal force, as schematically illustrated in **Figure 2a**. One main benefit of the spin coating process is its capacity of dense coating of uniform and thin films onto rigid flat surfaces. This ability is quite attuned along the requirement of excellent TEs, as the thickness of TEs needs to be optimized. It is an attractive method to fabricate transparent thin

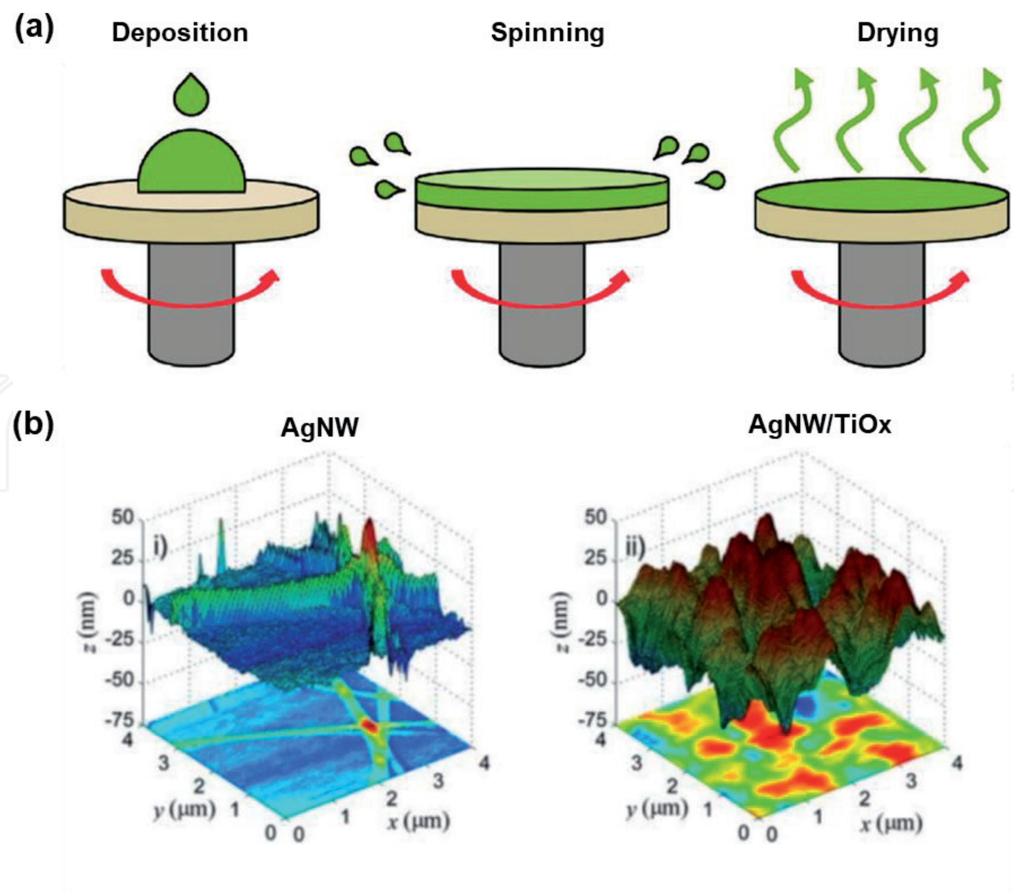

Figure 2.
(a) Schematic illustration of spin coating process. (b) AFM topographies of silver NW TEs without (left) and with the TiOx buffer layer (right). Reproduced with permission from Ref. [32].

graphene films (few nanometer-thick), as the optical transparency of these films will decline considerably with increase in thickness. For instance, each graphene layer absorbs 2.3% of white light. [117] Therefore, graphene-based TEs needs to be ultra-thin to obtain appropriate optical transmittance. Thin (3.1 nm) graphene TEs are fabricated using spin-coated for realizing OSCs. [118] Occasionally, the smoothness of spin-coated TEs is not perfect because of the material properties itself. For instance, silver NWs have decent dispersion in isopropanol, water, and few other frequently employed solvents and therefore can be easily spin coated on several substrates for the fabrication of TEs. Conversely, the spin coated silver NWs typically creates a nano-mesh (with certain thickness) on the substrates, making roughness for the subsequent processing, and therefore limits the applications of bottom TEs. In addition to the roughness concern, the weak silver NW/substrates adhesion causes mechanical failure of the devices, particularly in soft electronics. [88] This issue is resolved by spin coating a TiO_x buffer layer (~200 nm) over the silver NWs to get a comparatively uniform film, as displayed in **Figure 2b**. [32] Despite such potential, spin coating process have few limitations for the realizing of soft TEs. First, flatness of the spin-coated TEs is typically sensitive to spin speed, humidity, and substrate cleanness, which make the processing difficult to reproduce in ambient environment. Second, spin coating on large-area substrates is precisely difficult as it is challenging to clamp a hefty substrate and keep it stable at a high rotating speed. As a result, the spin coated films thickness is spatially different over a large substrate due to the variation of the localized centrifugation speed. Third, majority of the material is spun-off the substrate in spin coating, making this material-wasting approach. Bearing in mind, major portion of the total price of the raw materials of the soft electronic devices comprises of the material cost of TEs alone. Therefore, this wastage of material by spin coating is not financially viable for industrial mass-production, even though partially this may be reused.

5.2 Spray deposition

It is a coating process that uses a spray of particles or droplets to deposit a material onto a substrate using a nozzle, as schematically illustrated in **Figure 3a**. The spray nozzle creates a spray that comprises small drops of TE material and leads the materials transportation to the substrate by the help of carrier gas or electric charge. [119] Compared with other vacuum-free deposition techniques, the main benefit of spray coating is its capability of uniform coating of materials on non-flat substrates. **Figure 3b** displays organic photodetector (fiber-based) using PEDOT:PSS TE, that was realized using spray coating. it difficult to coat smooth PEDOT:PSS film though spin coating on the curved optical fiber surface. [120] It is also useful for subsequent processing, for instance, to spray coat on uneven surfaces, for instance, metal NWs, metal mesh coated substrates, as spin-coating of solutions can create non-continuous surface coverage. [33] Besides condense and smooth TCO-free films, spray coating has also the capability to deposit TCO films. **Figure 3c** shows

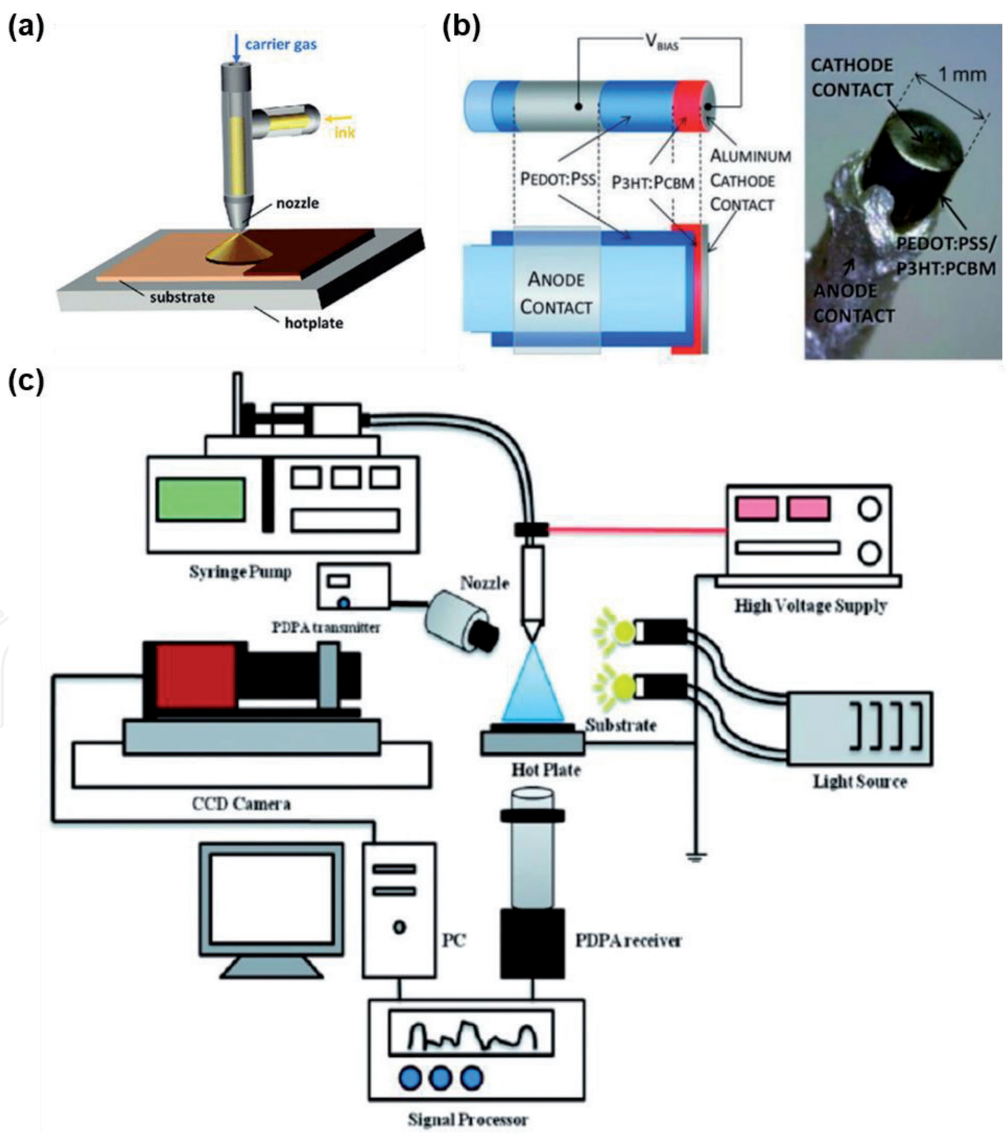

Figure 3.
(a) Schematic illustration of spray coating process. (b) Schematic (left) and photo (right) of fiber-based organic photodetector produced by spray coating. Reproduced with permission from Ref. [120] (c) schematic illustration of electrospray system. Reproduced with permission from Ref. [121].

the electrospray setup, utilized for deposition of zinc oxide (ZnO) and aluminum doped zinc oxide (AZO) films. [121] Despite such capabilities, spray processed TEs has the scalability problem, much more prominent as compared with other vacuum-free coating techniques. This limitation of low throughput has hammered its widespread adoption for production of large area soft TEs.

5.3 Inkjet printing

It is another highly used technique for making soft TEs. Inkjet printing is devised from dispenser printing where ink droplets exit the nozzles by a vibrant practice. By controlling the contraction expansion of the piezoelectric actuator, discrete ink drops are ejected from the nozzle making the anticipated design on top of the substrate, as schematically illustrated in **Figure 4a**. It is direct printing technique for high-resolution patterning, without the need of lithography other advantage key advantages that the printed design can be easily changed by modifying the digital pattern that controls the actuator. [122] Inkjet printing is an effective approach to producing large area soft TEs. **Figure 4b** displays a large-area organic solar cell (OSC) having silver current collecting mesh fabricated by inkjet-printing. The printed silver mesh consisted only small portion (~8%) of the total substrate area due to the mesh relatively small line width (~160 μm). The thickness of the printed silver mesh lines was >2 μm, which caused large height variation for the subsequent processing i.e. spin-coating of PEDOT:PSS and other active materials of the solar cell. This problem was resolved by embedding the silver mesh into an extra barrier film. The large-area OSCs having flexible Ag/PEDOT:PSS mesh TEs shown excellent performance as compared to that of TCO-solar cell, due to the high conductivity (sheet resistance ~1 Ω/□) of the silver mesh. [87] Inkjet printing processes based on mechanisms other than piezoelectric actuation are also utilized

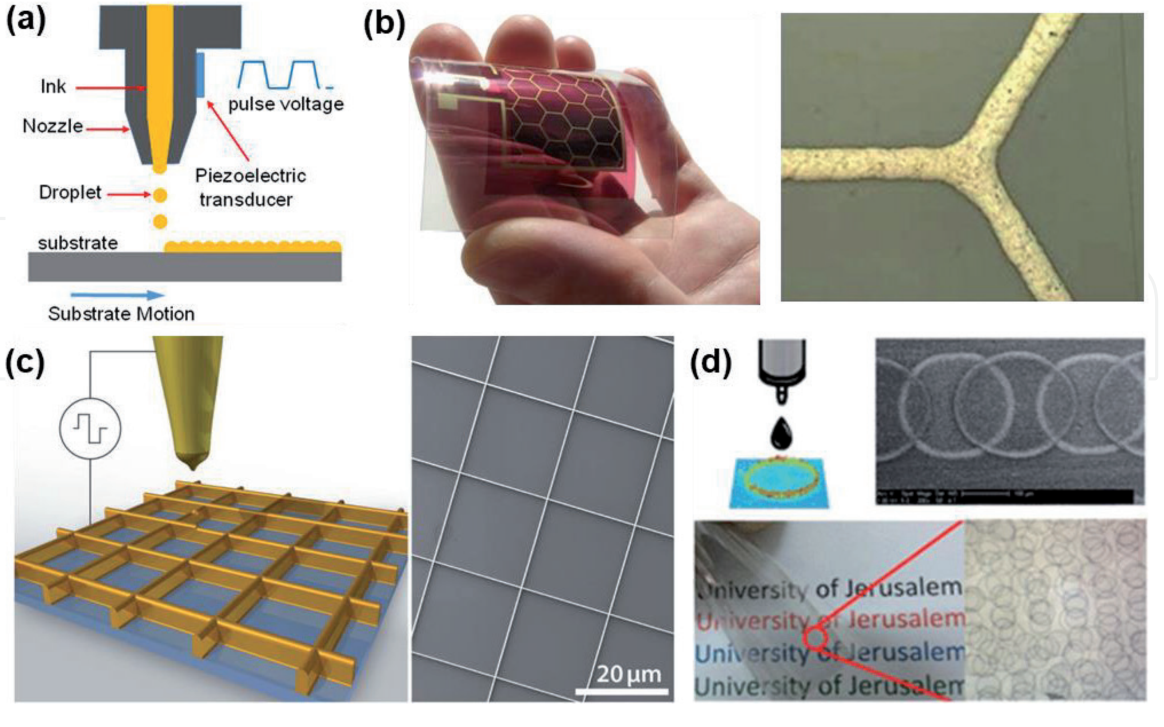

Figure 4.
(a) Schematic illustration of inkjet printing process. Reproduced with permission from Ref. [34]. (b) Photographs of inkjet-printed silver current mesh for large-area OSCs. Reproduced with permission from Ref. [87]. (c) Schematic illustration of high-aspect ratio metal grid along with electrohydrodynamic inkjet printing and the SEM image of the printed gold metal mesh electrode. Reproduced with permission from Ref. [65] (d) schematic diagram, SEM image, and photographs of the inkjet printed CNTs based TEs by "coffee ring effect". Reproduced with permission from Ref. [123].

for fabricating TEs. For instance, electrohydrodynamic inkjet process, as shown in **Figure 4c**, enabled the printing of high resolution gold meshes (feature size line 80 to 500 nm line widths) for realizing high performance TEs (8 Ω/□ at 94% optical transmittance), that can be custom-made for the application in different electronic devices. [65]

One major obstacle in attaining uniform inkjet printed structures is the coffee-ring effect, that initiates because of the capillary flow in the solvent evaporation step. [124] Though, this effect is also occasionally useful for making TEs with particular ring shapes. [125] **Figure 4d** demonstrates a CNTs based TE having joined ring patterns, that was made through inkjet printing the CNT ink on top of a pre-heated PET film. The height and diameter of the rings were the functions of applied temperature. Post heat-curing further lowered the sheet resistance of the CNT coatings. [123]

5.4 Screen printing

It is one of the attractive methods used to print soft TEs. In this technique, viscous inks are forced across stencils or patterned mesh (typically used as the template) using a scraper as shown in **Figure 5a**. The density of the used mesh and ink viscosity define the printing resolution and thickness of the pattern. [35] This handy and relatively simple technique is utilized mainly for graphene and PEDOT:PSS, however metals can also be printed. The resolution of conventional screen printing processes is not high, however, it can be improved to tens of micrometer using an improved screen-offset approach. [126] **Figure 5b** displays the screen printed graphite oxide (GO) arrays on PET film, which was afterwards reduced to rGO using hydriodic acid (HI) in modest environments. This technique developed an easy way to manufacture large-area graphene TEs (patterned), having thickness of few hundred nanometers. [127] Similar to other screen printable materials, mesh-patterned PEDOT:PSS TEs can be realized with various width/period ratios by adjusting the wire diameter, mesh size, and photoresist thickness. [128] Beside graphene and PEDOT:PSS, screen printing is also utilized for the patterning of metallic inks. **Figure 5c** shows the schematic illustration of the structure of OSC having printed silver mesh as TEs. This work relates the screen printed hybrid TEs having PEDOT:PSS on top of silver mesh with various other printing approaches for

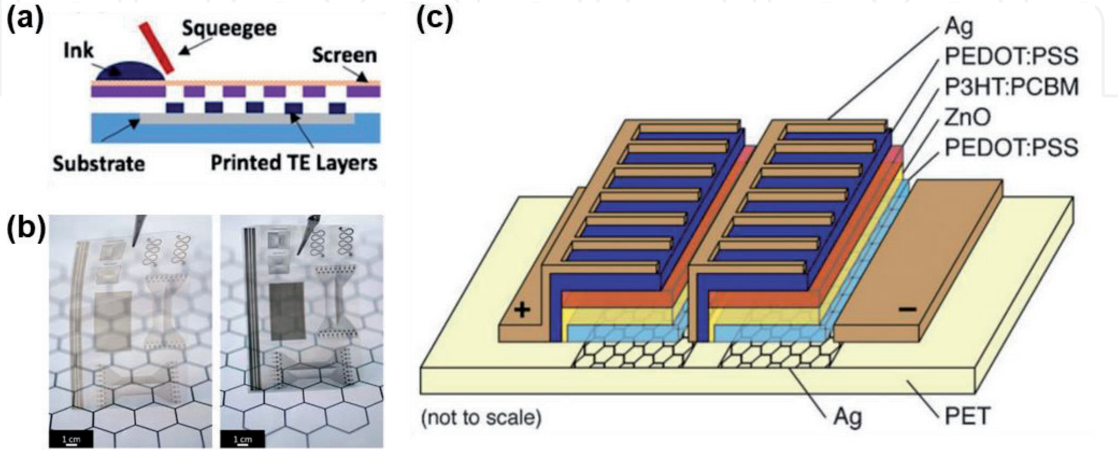

Figure 5.
(a) Schematic illustration of screen printing process. Reproduced with permission from Ref. [35]. (b) Photographs of GO (left) and rGO (right) films, fabricated by screen printing. Reproduced with permission from Ref. [127]. (c) Schematic illustration of the OSCs containing the layers of P3HT:PCBM, ZnO, PEDOT:PSS, and silver electrodes. The back silver electrode is printed by various processes including screen printing. Reproduced with permission from Ref. [129].

the vacuum-free and TCO free OSCs. It concludes that the uniformity of screen-printed silver meshes was superior as compared to inkjet printed and flexographic printed TEs, which were damaged by de-wetting in the subsequent PEDOT:PSS film processing. Consequently, the OSCs having screen-printed silver TEs showed better performance equated with inkjet printed and flexographic printed solar cells. [129]

5.5 Transfer printing

Transfer printing is an emergent method for fabrication of soft TEs, that empowers the processing of various materials into the chosen useful shapes. This produces manufacturing prospects in the field of soft electronics with comparable performance to that of traditional wafer-based processes, however with capacity to be deformed. In this technique, first the materials structures are fabricated on the conventional donor substrate and then wisely transferred onto unconventional soft substrates, as described in **Figure 6a**. [36] For instance, graphene ultra-thin films are first coated on Ni or Cu foils using the standard chemical vapor deposition (CVD) technique. [130] In order to be used as TEs, the this graphene has to be transferred directly to top of the devices or transparent substrates. There are two different transfer approaches (wet transfer and dry transfer) to transfer CVD graphene onto various soft substrates, as shown in **Figure 6b**. In wet transfer,

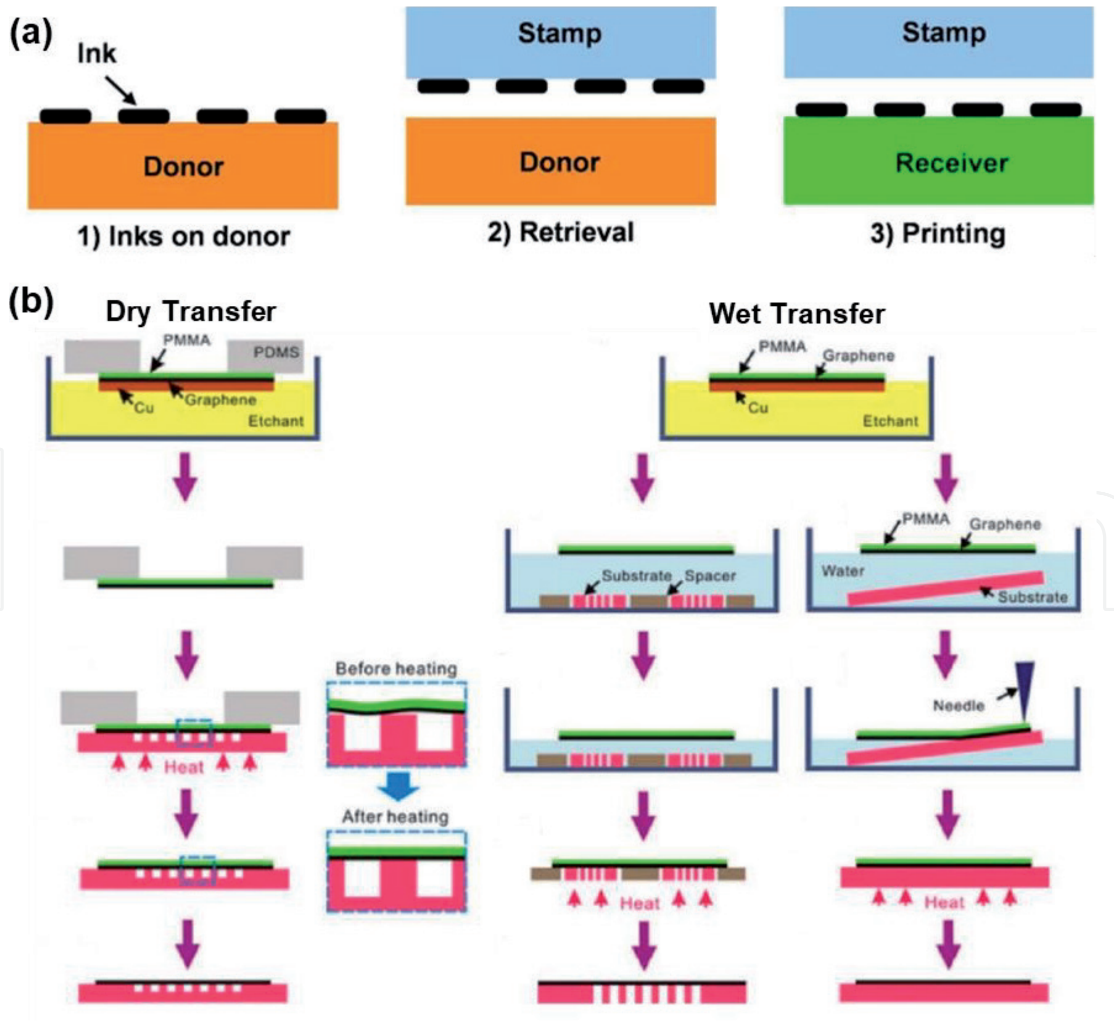

Figure 6.
(a) Schematic illustration of the transfer printing technique. Reproduced with permission from Ref. [36]. (b) Schematics of wet (right) and dry (lift) transfer printing for graphene soft TEs fabrication. Reproduced with permission from Ref. [131].

the graphene was initially covered by a PMMA thin film. Next, the underneath Cu film was removed by an etching step in $FeCl_3$. The graphene film covered by PMMA was then lifted-off either using a PDMS stamp for transfer, or directly picked up using the target substrate itself. [131] To enhance the throughput and production speed, transfer printing has been integrated with R2R process for the fabrication of large-area graphene (30-in) soft TEs. [105] Despite such potential, wet transfer has a limitation for the fabrication of top graphene-based TEs for the soft thin-film devices as the functional materials used in these devices are sensitive to moisture. To overcome this a dry transfer approach is developed, where a the film is directly coated on the PDMS stamps before transfer. [132] Besides graphene, other major transfer printable material for soft TEs is the metal nanowire/mesh films. These films typically have weak adhesion with the transfer substrates. This poor adhesion between the transfer substrates and metal films makes it easier to lift these films up with the PDMS, or another sticky polymeric stamp/target substrate. [60, 69] The high optical transmittance and superior conductivity of fabricated soft TEs using transfer printing ensure the high performance of soft electronic devices. [15, 60, 69, 70]

5.6 Slot-die coating

It is an effective process for printing one-dimensional structures. Slot-die coating is typically integrated with the R2R system for rapid production of soft electronic devices. As shown in **Figure 7a** and **b**, the solution is pushed out of the slot-die using a pneumatic scheme, and the solution is printed laterally in the

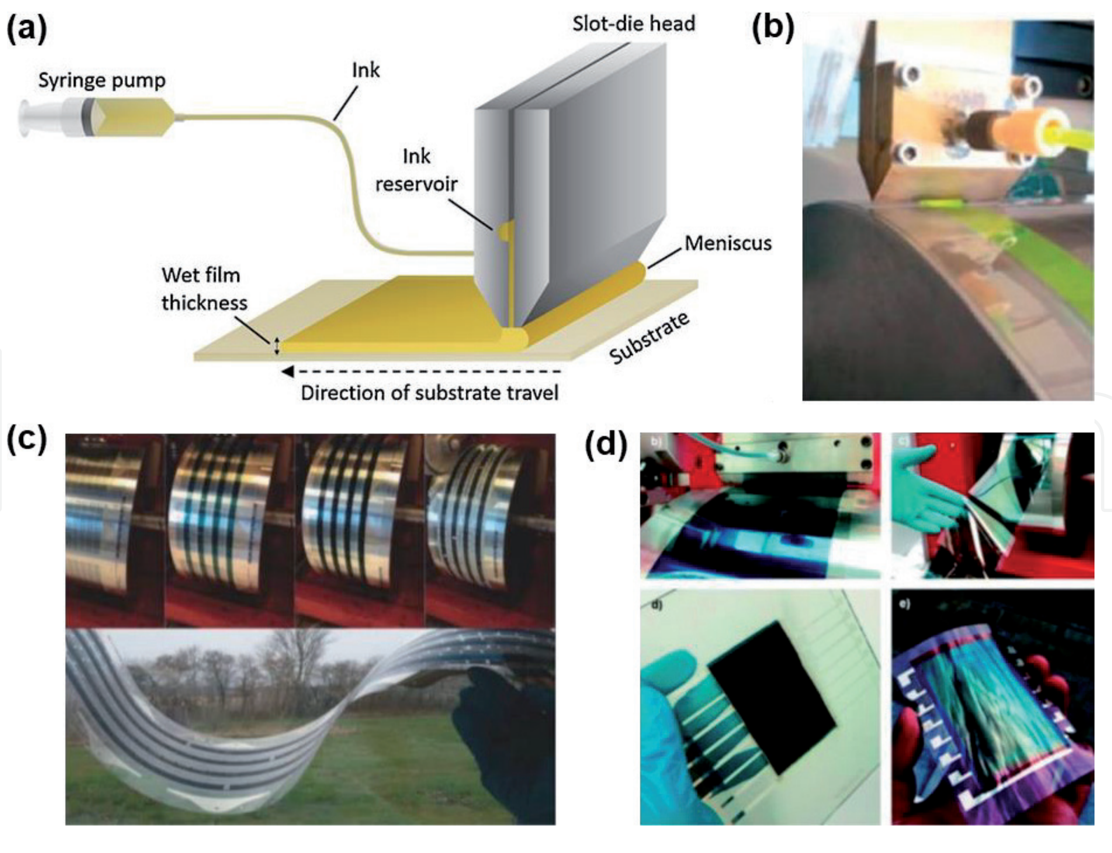

Figure 7.
(a) Schematic illustration of the slot-die coating technique. Reproduced with permission from Ref. [37] (b) photograph of the slot-die coating system. Reproduced with permission from Ref. [133] (c) photographs of the large-area soft OCSs having PEDOT:PSS TEs fabricated by slot-die coating. Reproduced with permission from Ref. [134] (d) photographs of the OCSs with high geometric fill factor. The employed PEDOT:PSS TEs are fabricated by slot-die coating. Reproduced with permission from Ref. [135].

direction of the moving head. The thickness of the printed structure is typically determined through the solution's concentration and it's flow rate, while the head speed controls the speed of printing. PEDOT:PSS is the most commonly processed TE material for slot-die coating. **Figure 7c** and **d** display flexible large-area OSCs, where, the PEDOT:PSS TEs and the organic active material were both printed by slot-die coating. [134] Key benefit of using slot-die coating is its capability to print on large-area substrates, as in slot-die coated films the center-to-edge thickness difference is negligible. Therefore, large-area OSCs having a high geometric fill factor (98.5%) were realized through integrating laser patterning with slot-die coating. [135] Besides PEDOT:PSS, slot-die coating has been effectively utilized for other conductive inks including silver NWs, [136] CNTs, [137] and graphene. [138] Similar to other processes, slot-die coating has also few limitations including, the harsh requirements regarding inks rheology for high quality coatings [139] and the existence of high density printing defects such as ribbing and rivulet. [140]

6. Conclusions

Recent progress of the development of vacuum-free TEs for soft electronics has been promising. This chapter presents a detailed overview on the latest advances of the vacuum-free soft TEs, comprising the introduction of electrode materials classes, the optical, electrical, mechanical, and surface features of the soft TEs. The chapter summarizes the vacuum-free techniques for the fabrication of soft TEs. Regardless of all the shortcomings discussed, we are optimistic that the vacuum-free TEs be going to play vital roles in soft electronic industries in the future.

Acknowledgements

This work was supported by the Qatar National Research Fund (a member of Qatar Foundation) under grant NPRP11S-0110-180246. The findings herein reflect the work and are solely the responsibility of the authors.

Conflict of interest

Authors declare no conflict of interests.

Author details

Arshad Khan*, Shawkat Ali, Saleem Khan, Moaaz Ahmed, Bo Wang and Amine Bermak
Division of Information and Computing Technology, College of Science and Engineering, Hamad Bin Khalifa University, Qatar Foundation, Doha, Qatar

*Address all correspondence to: arkhan4@hbku.edu.qa

References

[1] Hecht DS, Hu L, Irvin G. Emerging Transparent Electrodes Based on Thin Films of Carbon Nanotubes, Graphene, and Metallic Nanostructures. Advanced Materials. 2011;23:1482-513.

[2] Yu Z, Li L, Zhang Q, Hu W, Pei Q. Silver Nanowire-Polymer Composite Electrodes for Efficient Polymer Solar Cells. Advanced Materials. 2011;23:4453-7.

[3] deb SK, Lee S, Edwin Tracy C, Roland Pitts J, Gregg BA, Branz HM. Stand-alone photovoltaic-powered electrochromic smart window. Electrochimica Acta. 2001;46: 2125-30.

[4] Wu J, Agrawal M, Becerril HA, Bao Z, Liu Z, Chen Y, et al. Organic Light-Emitting Diodes on Solution-Processed Graphene Transparent Electrodes. ACS Nano. 2010;4:43-8.

[5] Blake P, Brimicombe PD, Nair RR, Booth TJ, Jiang D, Schedin F, et al. Graphene-Based Liquid Crystal Device. Nano Letters. 2008;8:1704-8.

[6] Cai J, Zhang C, Khan A, Liang C, Li W-D. Highly transparent and flexible polyaniline mesh sensor for chemiresistive sensing of ammonia gas. RSC Advances. 2018;8:5312-20.

[7] Wang J, Liang M, Fang Y, Qiu T, Zhang J, Zhi L. Rod-Coating: Towards Large-Area Fabrication of Uniform Reduced Graphene Oxide Films for Flexible Touch Screens. Advanced Materials. 2012;24:2874-8.

[8] Gordon RG. Criteria for Choosing Transparent Conductors. MRS Bulletin. 2000;25:52-7.

[9] Ellmer K. Past achievements and future challenges in the development of optically transparent electrodes. Nat Photon. 2012;6:809-17.

[10] Minami T. Transparent conducting oxide semiconductors for transparent electrodes. Semiconductor Science and Technology. 2005;20:S35-S44.

[11] Zhang Y, Ng S-W, Lu X, Zheng Z. Solution-Processed Transparent Electrodes for Emerging Thin-Film Solar Cells. Chemical Reviews. 2020;120:2049-122.

[12] Kumar A, Zhou C. The Race To Replace Tin-Doped Indium Oxide: Which Material Will Win? ACS Nano. 2010;4:11-4.

[13] Cairns DR, Witte RP, Sparacin DK, Sachsman SM, Paine DC, Crawford GP, et al. Strain-dependent electrical resistance of tin-doped indium oxide on polymer substrates. Applied Physics Letters. 2000;76:1425-7.

[14] Bel Hadj Tahar R, Ban T, Ohya Y, Takahashi Y. Tin doped indium oxide thin films: Electrical properties. Journal of Applied Physics. 1998;83:2631-45.

[15] Khan A, Liang C, Huang Y-T, Zhang C, Cai J, Feng S-P, et al. Template-Electrodeposited and Imprint-Transferred Microscale Metal-Mesh Transparent Electrodes for Flexible and Stretchable Electronics. Advanced Engineering Materials. 2019;21:1900723.

[16] Khan A, Lee S, Jang T, Xiong Z, Zhang C, Tang J, et al. High-Performance Flexible Transparent Electrode with an Embedded Metal Mesh Fabricated by Cost-Effective Solution Process. Small. 2016;12:3021-30.

[17] Bonaccorso F, Sun Z, Hasan T, Ferrari AC. Graphene photonics and optoelectronics. Nat Photon. 2010;4:611-22.

[18] Zhang M, Fang S, Zakhidov AA, Lee SB, Aliev AE, Williams CD, et al.

Strong, Transparent, Multifunctional, Carbon Nanotube Sheets. Science. 2005;309:1215-9.

[19] Kirchmeyer S, Reuter K. Scientific importance, properties and growing applications of poly(3,4-ethylenedioxythiophene). Journal of Materials Chemistry. 2005;15:2077-88.

[20] Vosgueritchian M, Lipomi DJ, Bao Z. Highly Conductive and Transparent PEDOT:PSS Films with a Fluorosurfactant for Stretchable and Flexible Transparent Electrodes. Advanced Functional Materials. 2012;22:421-8.

[21] De S, Higgins TM, Lyons PE, Doherty EM, Nirmalraj PN, Blau WJ, et al. Silver Nanowire Networks as Flexible, Transparent, Conducting Films: Extremely High DC to Optical Conductivity Ratios. ACS Nano. 2009;3:1767-74.

[22] van de Groep J, Spinelli P, Polman A. Transparent Conducting Silver Nanowire Networks. Nano Letters. 2012;12:3138-44.

[23] Hong S, Yeo J, Kim G, Kim D, Lee H, Kwon J, et al. Nonvacuum, Maskless Fabrication of a Flexible Metal Grid Transparent Conductor by Low-Temperature Selective Laser Sintering of Nanoparticle Ink. ACS Nano. 2013;7:5024-31.

[24] Wu H, Kong D, Ruan Z, Hsu P-C, Wang S, Yu Z, et al. A transparent electrode based on a metal nanotrough network. Nat Nano. 2013;8:421-5.

[25] Han B, Pei K, Huang Y, Zhang X, Rong Q, Lin Q, et al. Uniform Self-Forming Metallic Network as a High-Performance Transparent Conductive Electrode. Advanced Materials. 2014;26:873-7.

[26] Kim H-J, Lee S-H, Lee J, Lee E-S, Choi J-H, Jung J-H, et al. High-Durable AgNi Nanomesh Film for a Transparent Conducting Electrode. Small. 2014;10:3767-74.

[27] Kiruthika S, Gupta R, Rao KDM, Chakraborty S, Padmavathy N, Kulkarni GU. Large area solution processed transparent conducting electrode based on highly interconnected Cu wire network. Journal of Materials Chemistry C. 2014;2:2089-94.

[28] Choi H-J, Choo S, Jung P-H, Shin J-H, Kim Y-D, Lee H. Uniformly embedded silver nanomesh as highly bendable transparent conducting electrode. Nanotechnology. 2015;26:055305.

[29] Zhijun W, Shufen C, Huishan Y, Yi Z, Jingying H, Shiyong L. Top-emitting organic light-emitting devices based on silicon substrate using Ag electrode. Semiconductor Science and Technology. 2004;19:1138.

[30] Peng H, Zhu X, Sun J, Xie Z, Xie S, Wong M, et al. Efficient organic light-emitting diode using semitransparent silver as anode. Applied Physics Letters. 2005;87:173505.

[31] Gu D, Zhang C, Wu Y-K, Guo LJ. Ultrasmooth and Thermally Stable Silver-Based Thin Films with Subnanometer Roughness by Aluminum Doping. ACS Nano. 2014;8:10343-51.

[32] Leem D-S, Edwards A, Faist M, Nelson J, Bradley DDC, de Mello JC. Efficient Organic Solar Cells with Solution-Processed Silver Nanowire Electrodes. Advanced Materials. 2011;23:4371-5.

[33] Choi DY, Kang HW, Sung HJ, Kim SS. Annealing-free, flexible silver nanowire–polymer composite electrodes via a continuous two-step spray-coating method. Nanoscale. 2013;5:977-83.

[34] Lin X, Kavalakkatt J, Lux-Steiner MC, Ennaoui A. Inkjet-

Printed Cu2ZnSn(S, Se)4 Solar Cells. Advanced Science. 2015;2:1500028.

[35] Shin S, Kumar R, Roh JW, Ko D-S, Kim H-S, Kim SI, et al. High-Performance Screen-Printed Thermoelectric Films on Fabrics. Scientific Reports. 2017;7:7317.

[36] Linghu C, Zhang S, Wang C, Song J. Transfer printing techniques for flexible and stretchable inorganic electronics. npj Flexible Electronics. 2018;2:26.

[37] Patidar R, Burkitt D, Hooper K, Richards D, Watson T. Slot-die coating of perovskite solar cells: An overview. Materials Today Communications. 2020;22:100808.

[38] Groenendaal L, Jonas F, Freitag D, Pielartzik H, Reynolds JR. Poly(3,4-ethylenedioxythiophene) and Its Derivatives: Past, Present, and Future. Advanced Materials. 2000;12:481-94.

[39] Wald G. The Receptors of Human Color Vision. Action spectra of three visual pigments in human cones account for normal color vision and color-blindness. 1964;145:1007-16.

[40] Gao T, Li Z, Huang P-s, Shenoy GJ, Parobek D, Tan S, et al. Hierarchical Graphene/Metal Grid Structures for Stable, Flexible Transparent Conductors. ACS Nano. 2015;9:5440-6.

[41] Zhang D, Wang R, Wen M, Weng D, Cui X, Sun J, et al. Synthesis of Ultralong Copper Nanowires for High-Performance Transparent Electrodes. Journal of the American Chemical Society. 2012;134:14283-6.

[42] Rathmell AR, Bergin SM, Hua Y-L, Li Z-Y, Wiley BJ. The Growth Mechanism of Copper Nanowires and Their Properties in Flexible, Transparent Conducting Films. Advanced Materials. 2010;22:3558-63.

[43] Tokuno T, Nogi M, Jiu J, Sugahara T, Suganuma K. Transparent Electrodes Fabricated via the Self-Assembly of Silver Nanowires Using a Bubble Template. Langmuir. 2012;28:9298-302.

[44] Guo H, Lin N, Chen Y, Wang Z, Xie Q, Zheng T, et al. Copper Nanowires as Fully Transparent Conductive Electrodes. Scientific Reports. 2013;3:2323.

[45] Yu Z, Zhang Q, Li L, Chen Q, Niu X, Liu J, et al. Highly Flexible Silver Nanowire Electrodes for Shape-Memory Polymer Light-Emitting Diodes. Advanced Materials. 2011;23:664-8.

[46] Wang J, Yan C, Kang W, Lee PS. High-efficiency transfer of percolating nanowire films for stretchable and transparent photodetectors. Nanoscale. 2014;6:10734-9.

[47] Lee J, Lee P, Lee H, Lee D, Lee SS, Ko SH. Very long Ag nanowire synthesis and its application in a highly transparent, conductive and flexible metal electrode touch panel. Nanoscale. 2012;4:6408-14.

[48] Suh YD, Hong S, Lee J, Lee H, Jung S, Kwon J, et al. Random nanocrack, assisted metal nanowire-bundled network fabrication for a highly flexible and transparent conductor. RSC Advances. 2016;6:57434-40.

[49] Sciacca B, van de Groep J, Polman A, Garnett EC. Solution-Grown Silver Nanowire Ordered Arrays as Transparent Electrodes. Advanced Materials. 2016;28:905-9.

[50] Lee J-G, Kim D-Y, Lee J-H, Sinha-Ray S, Yarin AL, Swihart MT, et al. Production of Flexible Transparent Conducting Films of Self-Fused Nanowires via One-Step Supersonic Spraying. Advanced Functional Materials. 2017;27:1602548-n/a.

[51] Liu J-W, Wang J-L, Wang Z-H, Huang W-R, Yu S-H. Manipulating

Nanowire Assembly for Flexible Transparent Electrodes. Angewandte Chemie International Edition. 2014;53:13477-82.

[52] Gong S, Zhao Y, Yap LW, Shi Q, Wang Y, Bay JAPB, et al. Fabrication of Highly Transparent and Flexible NanoMesh Electrode via Self-assembly of Ultrathin Gold Nanowires. Advanced Electronic Materials. 2016;2:1600121-n/a.

[53] Wu H, Hu L, Rowell MW, Kong D, Cha JJ, McDonough JR, et al. Electrospun Metal Nanofiber Webs as High-Performance Transparent Electrode. Nano Letters. 2010;10:4242-8.

[54] Kang MG, Guo LJ. Nanoimprinted Semitransparent Metal Electrodes and Their Application in Organic Light-Emitting Diodes. Advanced Materials. 2007;19:1391-6.

[55] Guo CF, Sun T, Liu Q, Suo Z, Ren Z. Highly stretchable and transparent nanomesh electrodes made by grain boundary lithography. Nat Commun. 2014;5.

[56] Park JH, Lee DY, Kim Y-H, Kim JK, Lee JH, Park JH, et al. Flexible and Transparent Metallic Grid Electrodes Prepared by Evaporative Assembly. ACS Applied Materials & Interfaces. 2014;6:12380-7.

[57] Kang M-G, Joon Park H, Hyun Ahn S, Jay Guo L. Transparent Cu nanowire mesh electrode on flexible substrates fabricated by transfer printing and its application in organic solar cells. Solar Energy Materials and Solar Cells. 2010;94:1179-84.

[58] Kiruthika S, Rao KDM, Ankush K, Ritu G, Kulkarni GU. Metal wire network based transparent conducting electrodes fabricated using interconnected crackled layer as template. Materials Research Express. 2014;1:026301.

[59] Kang M-G, Kim M-S, Kim J, Guo LJ. Organic Solar Cells Using Nanoimprinted Transparent Metal Electrodes. Advanced Materials. 2008;20:4408-13.

[60] Zhang C, Khan A, Cai J, Liang C, Liu Y, Deng J, et al. Stretchable Transparent Electrodes with Solution-Processed Regular Metal Mesh for an Electroluminescent Light-Emitting Film. ACS Applied Materials & Interfaces. 2018;10:21009-17.

[61] Chen X, Nie S, Guo W, Fei F, Su W, Gu W, et al. Printable High-Aspect Ratio and High-Resolution Cu Grid Flexible Transparent Conductive Film with Figure of Merit over 80 000. Advanced Electronic Materials. 2019;5:1800991.

[62] Yonghee J, Jihoon K, Doyoung B. Invisible metal-grid transparent electrode prepared by electrohydrodynamic (EHD) jet printing. Journal of Physics D: Applied Physics. 2013;46:155103.

[63] Jang S, Jung W-B, Kim C, Won P, Lee S-G, Cho KM, et al. A three-dimensional metal grid mesh as a practical alternative to ITO. Nanoscale. 2016;8:14257-63.

[64] Huang Y, Bai X, Zhou M, Liao S, Yu Z, Wang Y, et al. Large-Scale Spinning of Silver Nanofibers as Flexible and Reliable Conductors. Nano Letters. 2016;16:5846-51.

[65] Schneider J, Rohner P, Thureja D, Schmid M, Galliker P, Poulikakos D. ElectrohydrodynamicNanoDripPrinting of High Aspect Ratio Metal Grid Transparent Electrodes. Advanced Functional Materials. 2016;26:833-40.

[66] Bai X, Liao S, Huang Y, Song J, Liu Z, Fang M, et al. Continuous Draw Spinning of Extra-Long Silver Submicron Fibers with Micrometer Patterning Capability. Nano Letters. 2017;17:1883-91.

[67] An S, Jo HS, Kim D-Y, Lee HJ, Ju B-K, Al-Deyab SS, et al. Self-Junctioned Copper Nanofiber Transparent Flexible Conducting Film via Electrospinning and Electroplating. Advanced Materials. 2016;28:7149-54.

[68] Xian Z, Han B, Li S, Yang C, Wu S, Lu X, et al. A Practical ITO Replacement Strategy: Sputtering-Free Processing of a Metallic Nanonetwork. Advanced Materials Technologies. 2017;2:1700061-n/a.

[69] Khan A, Huang Y-T, Miyasaka T, Ikegami M, Feng S-P, Li W-D. Solution-Processed Transparent Nickel-Mesh Counter Electrode with in-Situ Electrodeposited Platinum Nanoparticles for Full-Plastic Bifacial Dye-Sensitized Solar Cells. ACS Applied Materials & Interfaces. 2017;9:8083-91.

[70] Zhang C, Cai J, Liang C, Khan A, Li W-D. Scalable Fabrication of Metallic Nanofiber Network via Templated Electrodeposition for Flexible Electronics. Advanced Functional Materials. 2019;29:1903123.

[71] An BW, Gwak E-J, Kim K, Kim Y-C, Jang J, Kim J-Y, et al. Stretchable, Transparent Electrodes as Wearable Heaters Using Nanotrough Networks of Metallic Glasses with Superior Mechanical Properties and Thermal Stability. Nano Letters. 2016;16:471-8.

[72] Chen X, Guo W, Xie L, Wei C, Zhuang J, Su W, et al. Embedded Ag/Ni Metal-Mesh with Low Surface Roughness As Transparent Conductive Electrode for Optoelectronic Applications. ACS Applied Materials & Interfaces. 2017;9:37048-54.

[73] Jang J, Im H-G, Jin J, Lee J, Lee J-Y, Bae B-S. A Flexible and Robust Transparent Conducting Electrode Platform Using an Electroplated Silver Grid/Surface-Embedded Silver Nanowire Hybrid Structure. ACS Applied Materials & Interfaces. 2016;8:27035-43.

[74] Iwahashi T, Yang R, Okabe N, Sakurai J, Lin J, Matsunaga D. Nanoimprint-assisted fabrication of high haze metal mesh electrode for solar cells. Applied Physics Letters. 2014;105:223901.

[75] Gupta R, Rao KDM, Srivastava K, Kumar A, Kiruthika S, Kulkarni GU. Spray Coating of Crack Templates for the Fabrication of Transparent Conductors and Heaters on Flat and Curved Surfaces. ACS Applied Materials & Interfaces. 2014;6:13688-96.

[76] Zhou L, Xiang H-Y, Shen S, Li Y-Q, Chen J-D, Xie H-J, et al. High-Performance Flexible Organic Light-Emitting Diodes Using Embedded Silver Network Transparent Electrodes. ACS Nano. 2014;8:12796-805.

[77] Kang J, Jang Y, Kim Y, Cho S-H, Suhr J, Hong BH, et al. An Ag-grid/graphene hybrid structure for large-scale, transparent, flexible heaters. Nanoscale. 2015;7:6567-73.

[78] Hak-Jong C, Soyoung C, Pil-Hoon J, Ju-Hyeon S, Yang-Doo K, Heon L. Uniformly embedded silver nanomesh as highly bendable transparent conducting electrode. Nanotechnology. 2015;26:055305.

[79] Mao L, Chen Q, Li Y, Li Y, Cai J, Su W, et al. Flexible Silver Grid/PEDOT:PSS Hybrid Electrodes For Large Area Inverted Polymer Solar Cells. Nano Energy. 2014;10:259-67.

[80] Im H-G, Jeong S, Jin J, Lee J, Youn D-Y, Koo W-T, et al. Hybrid crystalline-ITO/metal nanowire mesh transparent electrodes and their application for highly flexible perovskite solar cells. Npg Asia Materials. 2016;8:e282.

[81] Zou J, Yip H-L, Hau SK, Jen AK-Y. Metal grid/conducting polymer hybrid

transparent electrode for inverted polymer solar cells. Applied Physics Letters. 2010;96:203301.

[82] Mayousse C, Celle C, Fraczkiewicz A, Simonato J-P. Stability of silver nanowire based electrodes under environmental and electrical stresses. Nanoscale. 2015;7:2107-15.

[83] Hsu P-C, Wang S, Wu H, Narasimhan VK, Kong D, Ryoung Lee H, et al. Performance enhancement of metal nanowire transparent conducting electrodes by mesoscale metal wires. Nat Commun. 2013;4.

[84] Bao W, Wan J, Han X, Cai X, Zhu H, Kim D, et al. Approaching the limits of transparency and conductivity in graphitic materials through lithium intercalation. Nat Commun. 2014;5.

[85] Ok JG, Kwak MK, Huard CM, Youn HS, Guo LJ. Photo–Roll Lithography (PRL) for Continuous and Scalable Patterning with Application in Flexible Electronics. Advanced Materials. 2013;25:6554-61.

[86] Au - Khan A, Au - Lee S, Au - Jang T, Au - Xiong Z, Au - Zhang C, Au - Tang J, et al. Scalable Solution-processed Fabrication Strategy for High-performance, Flexible, Transparent Electrodes with Embedded Metal Mesh. JoVE. 2017:e56019.

[87] Galagan Y, J.M. Rubingh J-E, Andriessen R, Fan C-C, W.M. Blom P, C. Veenstra S, et al. ITO-free flexible organic solar cells with printed current collecting grids. Solar Energy Materials and Solar Cells. 2011;95:1339-43.

[88] Lee J-Y, Connor ST, Cui Y, Peumans P. Solution-Processed Metal Nanowire Mesh Transparent Electrodes. Nano Letters. 2008;8:689-92.

[89] Yim JH, Joe S-y, Pang C, Lee KM, Jeong H, Park J-Y, et al. Fully Solution-Processed Semitransparent Organic Solar Cells with a Silver Nanowire Cathode and a Conducting Polymer Anode. ACS Nano. 2014;8:2857-63.

[90] Hauger TC, Al-Rafia SMI, Buriak JM. Rolling Silver Nanowire Electrodes: Simultaneously Addressing Adhesion, Roughness, and Conductivity. ACS Applied Materials & Interfaces. 2013;5:12663-71.

[91] Meng Y, Hu Z, Ai N, Jiang Z, Wang J, Peng J, et al. Improving the Stability of Bulk Heterojunction Solar Cells by Incorporating pH-Neutral PEDOT:PSS as the Hole Transport Layer. ACS Applied Materials & Interfaces. 2014;6:5122-9.

[92] Huo D, Kim MJ, Lyu Z, Shi Y, Wiley BJ, Xia Y. One-Dimensional Metal Nanostructures: From Colloidal Syntheses to Applications. Chemical Reviews. 2019;119:8972-9073.

[93] Dou L, Cui F, Yu Y, Khanarian G, Eaton SW, Yang Q, et al. Solution-Processed Copper/Reduced-Graphene-Oxide Core/Shell Nanowire Transparent Conductors. ACS Nano. 2016;10:2600-6.

[94] Chen Z, Ye S, Stewart IE, Wiley BJ. Copper Nanowire Networks with Transparent Oxide Shells That Prevent Oxidation without Reducing Transmittance. ACS Nano. 2014;8:9673-9.

[95] Hsu P-C, Wu H, Carney TJ, McDowell MT, Yang Y, Garnett EC, et al. Passivation Coating on Electrospun Copper Nanofibers for Stable Transparent Electrodes. ACS Nano. 2012;6:5150-6.

[96] Sajjad MT, Park J, Gaboriau D, Harwell JR, Odobel F, Reiss P, et al. CuSCN Nanowires as Electrodes for p-Type Quantum Dot Sensitized Solar Cells: Charge Transfer Dynamics and Alumina Passivation. The Journal of Physical Chemistry C. 2018;122:5161-70.

[97] Bulliard X, Ihn S-G, Yun S, Kim Y, Choi D, Choi J-Y, et al. Enhanced Performance in Polymer Solar Cells by Surface Energy Control. Advanced Functional Materials. 2010;20:4381-7.

[98] Khan A, Rahman K, Hyun M-T, Kim D-S, Choi K-H. Multi-nozzle electrohydrodynamic inkjet printing of silver colloidal solution for the fabrication of electrically functional microstructures. Appl Phys A. 2011;104:1113-20.

[99] Jo HS, An S, Lee J-G, Park HG, Al-Deyab SS, Yarin AL, et al. Highly flexible, stretchable, patternable, transparent copper fiber heater on a complex 3D surface. Npg Asia Materials. 2017;9:e347.

[100] Khan A. Novel Embedded Metal-mesh Transparent Electrodes: Vacuum-free Fabrication Strategies and Applications in Flexible Electronic Devices. Singapore: Springer Nature; 2020.

[101] Mattevi C, Eda G, Agnoli S, Miller S, Mkhoyan KA, Celik O, et al. Evolution of Electrical, Chemical, and Structural Properties of Transparent and Conducting Chemically Derived Graphene Thin Films. Advanced Functional Materials. 2009;19:2577-83.

[102] Park S, Lee K-S, Bozoklu G, Cai W, Nguyen ST, Ruoff RS. Graphene Oxide Papers Modified by Divalent Ions—Enhancing Mechanical Properties via Chemical Cross-Linking. ACS Nano. 2008;2:572-8.

[103] Reina A, Jia X, Ho J, Nezich D, Son H, Bulovic V, et al. Large Area, Few-Layer Graphene Films on Arbitrary Substrates by Chemical Vapor Deposition. Nano Letters. 2009;9:30-5.

[104] De S, King PJ, Lotya M, O'Neill A, Doherty EM, Hernandez Y, et al. Flexible, Transparent, Conducting Films of Randomly Stacked Graphene from Surfactant-Stabilized, Oxide-Free Graphene Dispersions. Small. 2010;6:458-64.

[105] Bae S, Kim H, Lee Y, Xu X, Park J-S, Zheng Y, et al. Roll-to-roll production of 30-inch graphene films for transparent electrodes. Nat Nano. 2010;5:574-8.

[106] Bae S-Y, Jeon I-Y, Yang J, Park N, Shin HS, Park S, et al. Large-Area Graphene Films by Simple Solution Casting of Edge-Selectively Functionalized Graphite. ACS Nano. 2011;5:4974-80.

[107] Baughman RH, Zakhidov AA, de Heer WA. Carbon Nanotubes--the Route Toward Applications. Science. 2002;297:787-92.

[108] Iijima S. Helical microtubules of graphitic carbon. Nature. 1991;354:56-8.

[109] Tasis D, Tagmatarchis N, Bianco A, Prato M. Chemistry of Carbon Nanotubes. Chemical Reviews. 2006;106:1105-36.

[110] Wu Z, Chen Z, Du X, Logan JM, Sippel J, Nikolou M, et al. Transparent, Conductive Carbon Nanotube Films. Science. 2004;305:1273-6.

[111] Jo JW, Jung JW, Lee JU, Jo WH. Fabrication of Highly Conductive and Transparent Thin Films from Single-Walled Carbon Nanotubes Using a New Non-ionic Surfactant via Spin Coating. ACS Nano. 2010;4:5382-8.

[112] Pint CL, Xu Y-Q, Moghazy S, Cherukuri T, Alvarez NT, Haroz EH, et al. Dry Contact Transfer Printing of Aligned Carbon Nanotube Patterns and Characterization of Their Optical Properties for Diameter Distribution and Alignment. ACS Nano. 2010;4:1131-45.

[113] Reuter AESKWLoUMK. PEDOT: Principles and Applications of an Intrinsically Conductive Polymer. FL: CRC Press,; 2010.

[114] Lipomi DJ, Lee JA, Vosgueritchian M, Tee BCK, Bolander JA, Bao Z. Electronic Properties of Transparent Conductive Films of PEDOT:PSS on Stretchable Substrates. Chemistry of Materials. 2012;24:373-82.

[115] Das TK, Prusty S. Review on Conducting Polymers and Their Applications. Polymer-Plastics Technology and Engineering. 2012;51:1487-500.

[116] Gangopadhyay R, De A. Conducting Polymer Nanocomposites: A Brief Overview. Chemistry of Materials. 2000;12:608-22.

[117] Nair RR, Blake P, Grigorenko AN, Novoselov KS, Booth TJ, Stauber T, et al. Fine Structure Constant Defines Visual Transparency of Graphene. Science. 2008;320:1308-.

[118] Wu J, Becerril HA, Bao Z, Liu Z, Chen Y, Peumans P. Organic solar cells with solution-processed graphene transparent electrodes. Applied Physics Letters. 2008;92:263302.

[119] Khan A, Rahman K, Kim DS, Choi KH. Direct printing of copper conductive micro-tracks by multi-nozzle electrohydrodynamic inkjet printing process. Journal of Materials Processing Technology. 2012;212:700-6.

[120] Binda M, Natali D, Iacchetti A, Sampietro M. Integration of an Organic Photodetector onto a Plastic Optical Fiber by Means of Spray Coating Technique. Advanced Materials. 2013;25:4335-9.

[121] Mahmood K, Swain BS, Jung HS. Controlling the surface nanostructure of ZnO and Al-doped ZnO thin films using electrostatic spraying for their application in 12% efficient perovskite solar cells. Nanoscale. 2014;6:9127-38.

[122] Khan A, Roo JS, Kraus T, Steimle J. Soft Inkjet Circuits: Rapid Multi-Material Fabrication of Soft Circuits using a Commodity Inkjet Printer. Proceedings of the 32nd Annual ACM Symposium on User Interface Software and Technology. New Orleans, LA, USA: Association for Computing Machinery; 2019. p. 341-54.

[123] Shimoni A, Azoubel S, Magdassi S. Inkjet printing of flexible high-performance carbon nanotube transparent conductive films by "coffee ring effect". Nanoscale. 2014;6:11084-9.

[124] Yunker PJ, Still T, Lohr MA, Yodh AG. Suppression of the coffee-ring effect by shape-dependent capillary interactions. Nature. 2011;476:308-11.

[125] Layani M, Gruchko M, Milo O, Balberg I, Azulay D, Magdassi S. Transparent Conductive Coatings by Printing Coffee Ring Arrays Obtained at Room Temperature. ACS Nano. 2009;3:3537-42.

[126] Fukuda K, Someya T. Recent Progress in the Development of Printed Thin-Film Transistors and Circuits with High-Resolution Printing Technology. Advanced Materials. 2017;29:1602736.

[127] Overgaard MH, Kühnel M, Hvidsten R, Petersen SV, Vosch T, Nørgaard K, et al. Highly Conductive Semitransparent Graphene Circuits Screen-Printed from Water-Based Graphene Oxide Ink. Advanced Materials Technologies. 2017;2:1700011.

[128] Zhou L, Yu M, Chen X, Nie S, Lai W-Y, Su W, et al. Screen-Printed Poly(3,4-Ethylenedioxythiophene):Poly(Styrenesulfonate) Grids as ITO-Free Anodes for Flexible Organic Light-Emitting Diodes. Advanced Functional Materials. 2018;28:1705955.

[129] Hösel M, Søndergaard RR, Angmo D, Krebs FC. Comparison of Fast Roll-to-Roll Flexographic, Inkjet, Flatbed, and Rotary Screen Printing of

Metal Back Electrodes for Polymer Solar Cells. Advanced Engineering Materials. 2013;15:995-1001.

[130] Novoselov KS, Fal'ko VI, Colombo L, Gellert PR, Schwab MG, Kim K. A roadmap for graphene. Nature. 2012;490:192-200.

[131] Suk JW, Kitt A, Magnuson CW, Hao Y, Ahmed S, An J, et al. Transfer of CVD-Grown Monolayer Graphene onto Arbitrary Substrates. ACS Nano. 2011;5:6916-24.

[132] You P, Liu Z, Tai Q, Liu S, Yan F. Efficient Semitransparent Perovskite Solar Cells with Graphene Electrodes. Advanced Materials. 2015;27:3632-8.

[133] Sandström A, Dam HF, Krebs FC, Edman L. Ambient fabrication of flexible and large-area organic light-emitting devices using slot-die coating. Nature Communications. 2012;3:1002.

[134] Cheng P, Bai H, Zawacka NK, Andersen TR, Liu W, Bundgaard E, et al. Roll-Coated Fabrication of Fullerene-Free Organic Solar Cells with Improved Stability. Advanced Science. 2015;2:1500096.

[135] Lucera L, Machui F, Kubis P, Schmidt HD, Adams J, Strohm S, et al. Highly efficient, large area, roll coated flexible and rigid OPV modules with geometric fill factors up to 98.5% processed with commercially available materials. Energy & Environmental Science. 2016;9:89-94.

[136] Kim D-J, Shin H-I, Ko E-H, Kim K-H, Kim T-W, Kim H-K. Roll-to-roll slot-die coating of 400 mm wide, flexible, transparent Ag nanowire films for flexible touch screen panels. Scientific Reports. 2016;6:34322.

[137] Shin K, Park J, Lee C. A 250-mm-width, flexible, and continuous roll-to-roll slot-die coated carbon nanotube/silver nanowire film fabrication and a study on the effect of anti-reflective overcoat. Thin Solid Films. 2016;598:95-102.

[138] Hu X, Meng X, Xiong J, Huang Z, Yang X, Tan L, et al. Roll-to-Roll Fabrication of Flexible Orientated Graphene Transparent Electrodes by Shear Force and One-Step Reducing Post-Treatment. Advanced Materials Technologies. 2017;2:1700138.

[139] Jakubka F, Heyder M, Machui F, Kaschta J, Eggerath D, Lövenich W, et al. Determining the coating speed limitations for organic photovoltaic inks. Solar Energy Materials and Solar Cells. 2013;109:120-5.

[140] Nam J, Carvalho MS. Flow visualization and operating limits of tensioned-web-over slot die coating process. Chemical Engineering and Processing: Process Intensification. 2011;50:471-7.